In vivo evaluation of a biodegradable magnesium implant

Ryo Maekawa[1], Yoshinobu Oka[1], Jumpei Natsui[1], Hiroaki Wada[1], Wook-Cheol Kim[2], Yusuke Hono[3], Sadami Tsutsumi[4], Takashi Koizumi[1], Shunji Yamada[1], Ken Ichi Matsuda[1], Kenji Takahashi[1]
[1]Kyoto Prefectural University of Medicine, Kyoto, Japan, [2] Uji Takeda Hospital, Kyoto, Japan,
[3] Kyoto Prefectural Technology Center for Small and Medium Enterprises, Kyoto, Japan,
[4] Kyoto University, Kyoto, Japan
Email of Presenting Author: maka@koto.kpu-m.ac.jp

Disclosures: Ryo Maekawa (N), Yoshinobu Oka (N), Junpei Natsui(N), Hiroaki Wada(N), Wook-Cheol Kim(N), Yusuke Hono(N), Sadami Tsutsumi(N), Ken Ichi Matsuda(N), Kenji Takahashi(N)

INTRODUCTION: Current biodegradable implants are not ideal in terms of degradation behavior and mechanical strength. Although magnesium (Mg) alloy implants have been developed, concerns persist regarding cytotoxic from alloying elements and heterogeneous microstructure. Pure Mg degrades rapidly in vivo, limiting its practical application; however, improving its corrosion resistance and mechanical strength could make it an ideal biodegradable implant. We developed biodegradable implants from high-purity Mg (HP-Mg) and have previously conducted both in vitro[1)] and in vivo[2)] evaluations. This study aimed to evaluate the in vivo efficacy and safety of these implants.

MATERIAL & METHODS: Twelve-week-old Japanese white rabbits were used to create three implantation models: intramedullary, transcortical, and intramuscular (n = 6 each), using 99.9% HP-Mg pins (φ2.0 mm) (Figure 1). Evaluations included changes in body weight, macroscopic findings, serum Ca, Mg, and inorganic phosphate (IP) levels, radiography, μCT, and histology. The soft tissue thickness of the lower leg was measured on anteroposterior plain radiographs. Implant degradation was assessed by calculating the residual implant volume on μCT images.

RESULTS: No abnormal findings were observed in body weight, macroscopic findings, or blood tests in any of the animals. Plain radiographs showed no gas accumulation or implant migration (Figure 2). The soft tissue thickness in each model decreased in the order: transcortical > intramedullary > intramuscular. At 12 weeks postoperatively, μCT (Figure 3) demonstrated good callus formation, with > 86% of the implant volume retained. No heterotopic ossification was observed. The maximum bending stress remained above 47% of the initial strength. Histology revealed implant dissolution and abundant osteoid formation.

DISCUSSION and CONCLUSION: HP-Mg implants exhibited favorable biocompatibility without serious adverse events observed in any model, and implant degradation and good callus formation were confirmed by imaging and histological assessment. At 12 weeks, the implants were still present, demonstrating that early degradation of high-purity Mg was avoided in vivo. These results support HP-Mg as a promising candidate for clinical translation, consistent with our previous in vitro studies. Future research will focus on further enhancing implant functionality while developing biodegradable implants with optimized degradation kinetics.

SIGNIFICANCE/CLINICAL RELEVANCE: This study demonstrates the potential of high-purity Mg implants with controlled degradation rates for clinical applications, offering a promising alternative to current biodegradable implants and addressing the limitations of Mg alloy implants.

REFERENCES: [1)] Ryo Maekawa. Efficacy of high-purity magnesium for biodegradable implants. Poster presented at: Orthopedic Research Society Annual Meeting; February 3, 2024; Long Beach, CA.
[2)] Ryo Maekawa. Evaluation of biodegradable metal implants with controlled dissolution rates in vivo. Poster presented at: Orthopedic Research Society Annual Meeting; February 8, 2025; Phoenix, AZ.

ACKNOWLEDGEMENTS: We gratefully acknowledge NITTOSEIKO CO., LTD. for their financial support through a collaborative research grant and for providing the high-purity magnesium materials used in this study.

Figure 1. Mg pin

Figure2. X-ray imaging

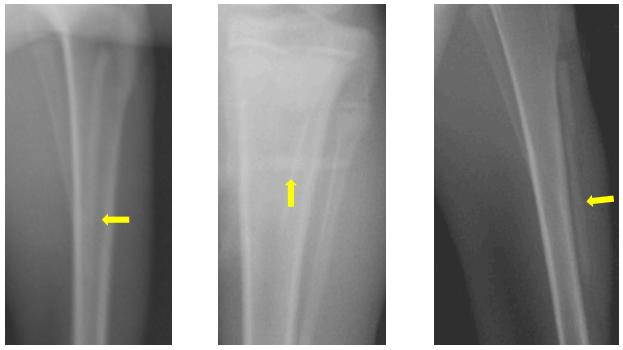

Figure 3. μ-CT imaging